ELSEVIER

Nuclear Instruments and Methods in Physics Research A 488 (2002) 175–183

NUCLEAR INSTRUMENTS & METHODS IN PHYSICS RESEARCH Section A

www.elsevier.com/locate/nima

Performance of a CMS silicon strip detector module with APV25 readout

M. Friedl*, T. Bauer, J. Hrubec, M. Krammer, M. Pernicka

Institute of High Energy Physics, Austrian Academy of Sciences, Nikolsdorfergasse 18, A-1050 Vienna, Austria

Received 28 August 2001; received in revised form 13 December 2001; accepted 17 December 2001

Abstract

The Compact Muon Solenoid experiment at the Large Hadron Collider at CERN will include a silicon strip tracker covering a sensitive area of 206 m^2 with about 10 million readout channels. Its silicon detectors, made from 6″ wafers, will be read out by APV25 front-end chips, fabricated in the 0.25 μm deep submicron process which is intrinsically radiation tolerant. A first prototype module has been built consisting of two chained silicon sensors of 320 μm thickness and three APV25 chips (version S0). The performance of this module has been evaluated in a pion and proton beam at the Paul Scherrer Institute (Villigen/CH).

PACS: 29.40.Gx; 29.40.Wk; 07.50.Qx

Keywords: APV25; Silicon; Detector; Module; Tracker; CMS

1. Introduction

In late 1999, the Compact Muon Solenoid (CMS) collaboration decided to change the design of the tracker, which was previously based on silicon strip detectors and micro-strip gas chambers, and to construct a silicon strip tracker with a total area of 206 m^2 [1,2]. The silicon sensors will mainly be made from 6″ wafers, resulting in a maximum strip length of 21 cm by chaining two sensors. In addition to the 320 μm thick detectors at smaller radii, sensors with 500 μm thickness will be used to compensate the additional noise of the long detectors in the outer part of the tracker by a higher energy deposition. The strip pitches vary between 80 and 205 μm.

The high particle rates at full Large Hadron Collider (LHC) operation and the resulting radiation levels in the tracker volume require the use of radiation-hard front-end electronics. The APV25 chip [3], designed to read out the CMS silicon strip detectors, is therefore manufactured in the industry-standard 0.25 μm technology, which is an economic alternative to expensive specialized radiation-tolerant processes by providing an intrinsic radiation hardness due to its thin gate oxides. The APV25 is a redesign of the APV6 prototype in 1.2 μm technology [4] with significantly improved noise characteristics and including additional features.

The APV25 chip will be driven synchronously by the LHC clock at 40 MHz. Each chip contains 128 channels with a preamplifier, a CR-RC shaper with a time constant of 50 ns and a 192-cell analog pipeline. The implemented deconvolution

*Corresponding author.
E-mail address: markus.friedl@cern.ch (M. Friedl).

0168-9002/02/$ - see front matter
PII: S0168-9002(02)00511-9

algorithm [5] narrows the pulses and thus allows to identify precisely the LHC bunch crossing from which a signal originates. After receiving a trigger signal, the analog data are multiplexed to the serial output line. Alternatively, the APV25 can be operated in peak mode without deconvolution or in a multi-peak mode, where for each trigger the signals of three consecutive time slots are presented at the output.

2. Experimental setup

Before producing strip detectors in larger quantities for CMS, it was of great interest to measure the characteristic parameters of a detector with realistic dimensions for minimum ionizing particles and at particle rates comparable to the future LHC operation.

The first silicon detector module with an APV25 readout (Fig. 1) was built at our institute in early 2000. It consisted of two sensors, made from 6″ wafers of 320 μm thickness, with a total strip length of 16.5 cm, a strip width of 34 μm and a strip pitch of 140 μm. The high silicon bulk resistivity resulted in a low depletion voltage of approximately 70 V. The detector module was partially read out by three APV25 chips (version S0), which were mounted on a dedicated printed circuit board (PCB) hybrid and connected to the sensors through a two-stage pitch adapter.

This APV25 detector module was tested at the Paul Scherrer Institute in a 350 MeV c^{-1} particle beam, delivering pions (which are almost minimum ionizing particles) and protons. For most of the measurements, the protons were removed by an aluminum shield in front of the bending magnets of the beamline. A scintillator counter (12×12 mm^2) behind the module was used to trigger on particles traversing approximately the center of the module. The module was operated in a cooling box at -10° C to provide conditions similar to CMS. As an exception, for the angle scan the module had to be run at ambient temperature due to mechanical constraints.

The APV25 chips were driven by the nominal LHC bunch crossing frequency of 40 MHz. A custom phase-locked loop circuit was developed to derive the APV clock from the 50 MHz PSI beam timing together with a synchronization pulse to select scintillator triggers which were in phase with both clocks. Most of the data have been taken at incident particle rates of about 10 kHz cm^{-2}. For a 24 h period of high intensity the beam was tuned to deliver particles at 1.4 MHz cm^{-2}, exceeding the expected particle rate at the innermost radius of the CMS silicon strip tracker during LHC operation.

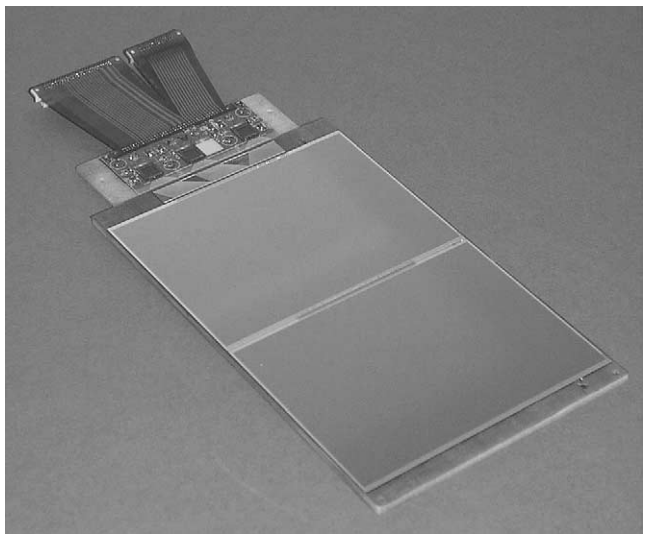

Fig. 1. The APV25 silicon strip detector module.

At our institute, a complete VME-based APV readout system [6] has been developed, including an APV sequencer, I^2C bus masters, 12-bit ADCs at 40 MHz and supporting hardware. Fig. 2 shows a schematic diagram of this setup. A comprehensive PC data acquisition software with online analysis communicated with the electronics. A second PC was used for slow controls and monitoring purposes, controlling the cooling system and the detector bias. An extended version of the data acquisition software was used for offline analysis. In every run, 600 random-triggered initial events were used for pedestal and noise evaluation, while the following events (typically 40k) were subjected to zero-suppression and clustering algorithms. All data were corrected for common-mode noise. For our analysis, we used cluster cuts of 6σ for the central seed strip and 3σ for the neighboring strips in terms of the strip RMS noise.

3. Results

3.1. Signal distribution

In Fig. 3, the distributions of cluster signals are shown for 350 MeV c^{-1} pions and protons. To fit the measured signal distribution of the pions, a Landau function was convoluted with a narrow Gaussian curve to account for electronic noise and intrinsic detector fluctuations. The distribution of the much higher signals of the protons can be almost completely described by a Gaussian function. The measured signals match very well with calculations of the restricted energy loss in silicon in the framework of the Bethe–Bloch theory. A calculated ratio of 6.0 between the mean energy loss of protons and pions compares to a measured quotient of 6.6.

3.2. Signal-to-noise ratio

The signal-to-noise ratio (SNR) is an important parameter for the detector efficiency. For the CMS silicon strip tracker modules, a most probable SNR > 10 is demanded throughout their lifetime for minimum ionizing particles, which ensures an efficiency close to 100%. Fig. 4 shows the most probable SNR obtained with the APV25 detector module in the pion beam as a function of the bias voltage for both peak and deconvolution modes. The equivalent noise charge (ENC) of the detector and amplifier system can be approximately derived by dividing the charge deposited by a minimum ionizing particle by the SNR. Table 1 compares the SNR and ENC values obtained with the APV25 detector module at full depletion to similar

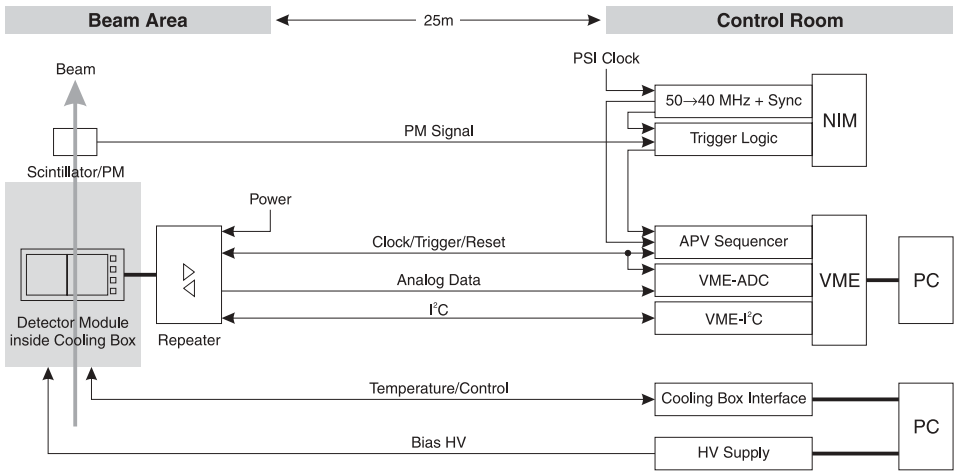

Fig. 2. Block diagram of the Vienna APV setup.

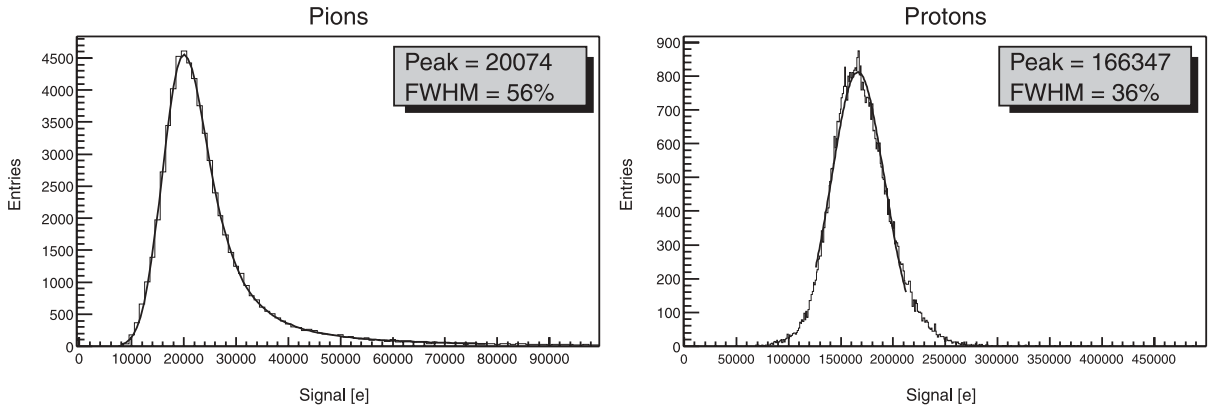

Fig. 3. Typical pion (left) and proton (right) signal distributions measured at a momentum of 350 MeV c^{-1} with the APV25 chips in deconvolution mode. In the proton picture, the x-axis range is five times larger than in the pion plot. The absolute charge scale has been obtained from internal calibration, which is accurate to about $\pm 20\%$.

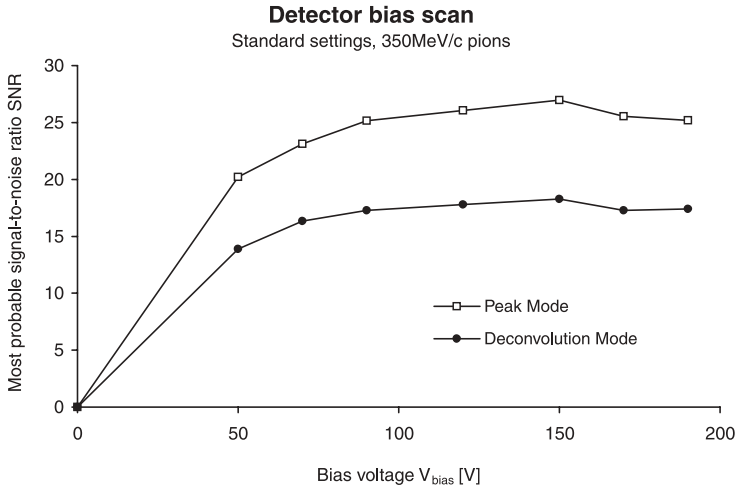

Fig. 4. SNR of the APV25 silicon detector module as a function of the detector bias for 350 MeV c^{-1} pions.

measurements performed with an APV6 readout [6].

The detector strip length determines the load capacitance seen by the amplifier and thus influences the electronic noise and the SNR. Moreover, the collected charge signal decreases with increasing irradiation due to the creation of crystal defects which act as charge traps. In addition, the detector noise increases with the rising leakage current, both effects leading to an

Table 1
Typical noise (ENC) and most probable signal-to-noise (SNR) values of non-irradiated, full-size CMS detector modules measured with 350 MeV c^{-1} pions

Mode	APV6		APV25	
	ENC [e]	SNR	ENC [e]	SNR
Peak	1400	16	900	25
Deconvolution	2250	10	1300	17

SNR reduction. Nevertheless, the APV25 performance offers sufficient margin to maintain excellent efficiency even after 10 years of LHC operation.

3.3. Module robustness

To check for a possible signal degradation along the strips, the scintillator behind the APV25 module was moved to several positions along the strip direction, by that defining different areas under test. As expected from the electrical properties of signal generation, no difference in the performance was obtained with respect to the position along the strip axis. As a particle crossing the detector represents a current source, the integral charge (which is measured by the amplifier) is not affected by varying the strip series resistance.

Driven by the APV clock at 40 MHz, sampled values of the APV25 shaper are stored for each readout channel in the chip-internal analog pipeline and retrieved up to 192 clock cycles (corresponding to 4.8 μs) later. By varying this latency time, neither signal nor noise was influenced, demonstrating the ability of the APV25 pipeline to hold the signal, without noticeable leakage, beyond the required CMS first-level trigger latency.

3.4. Optical link

The APV25 output signals were usually transmitted through a copper cable with a length of 25 m, but alternatively, a prototype of the CMS analog optical link [7] with 100 m of single-mode fiber, was installed for comparative measurements. The SNR obtained with the optical link was approximately 7% higher than with the copper cable. Although additional noise was introduced by the optical link, this effect was overcompensated by the significantly higher bandwidth compared to the copper cable used. Thus, the faster settling time of the signal obtained with optical readout improved the SNR.

The prototype optical link used in this test with the APV25 detector module had a higher gain and therefore a lower noise contribution compared to the optical link foreseen for the final tracker readout. Nevertheless, the final analog optical link is expected to contribute <850 e noise [8].

3.5. High intensity

During the 24-h period of high-intensity pion beam (1.4 MHz cm^{-2}), the detector performance remained unchanged in terms of signal and noise. However, the leakage current as shown in Fig. 5 increased as a linear function of the fluence accumulated in time. Initially, the current was very low, but jumps by approximately 0.5 μA as soon as the high-intensity beam was turned on. This is caused by the large number of charge carriers generated within the detector by the crossing pions, therefore it is known as beam-induced current.

The slope of the current in Fig. 5 corresponds to the increase of the leakage current I caused by radiation defects [9], which has been parameterized by

$$\Delta I = \alpha \Phi_{\mathrm{eq}} V \tag{1}$$

where α is the current related damage rate, Φ_{eq} the 1 MeV neutron equivalent fluence and V the sensitive volume. Without any annealing, a current-related damage rate of $\alpha \approx 8 \times 10^{-17}$ A cm^{-1} at room temperature can be derived from this measurement, which agrees with values given by the CERN RD48 (ROSE) collaboration [9].

Occasionally, the beam went off for a few seconds, resulting in a measurement of the pure leakage current without the beam-induced component. Joining these points would result in a parallel line with the same slope but at a lower level. The current spike at noon occurred due to a short power failure of the cooling system, resulting in a temporary current increase. After restoring the operating temperature, the current curve continues unaffected. Later, the beam intensity was slightly reduced for about 2 h, resulting in a lower beam-induced current.

3.6. Angle scan

In order to study the signal properties under non-perpendicular penetration by the beam

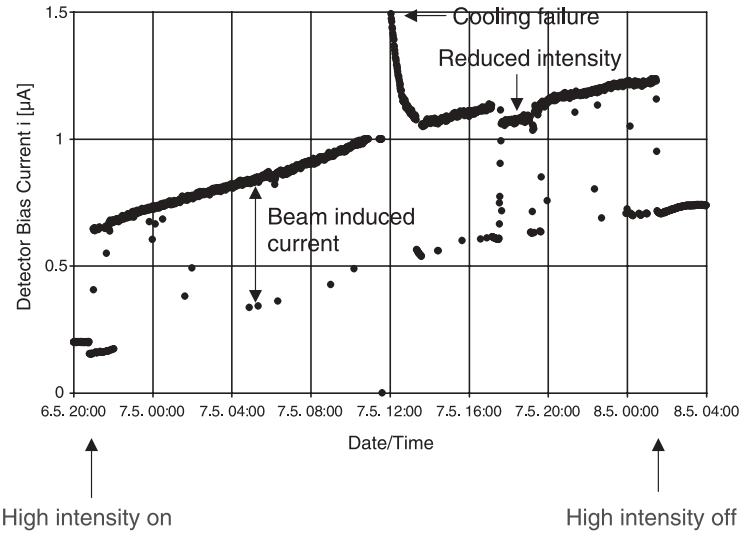

Fig. 5. Detector current of the APV25 module during the high-intensity period, see body text for a detailed description.

particles the APV25 detector module had to be rotated around its strip direction. Therefore these measurements were performed at room temperature outside the cooling box. Denoting the perpendicular incidence of the beam particles with $\alpha = 0^\circ$, the beam incidence angle α was varied in four steps up to 60°. Previous studies [10] have shown that due to the longer path of the beam particles in the detector, the total collected charge increases as given by

$$\frac{Q_\alpha}{Q_0} = \frac{1}{\cos\alpha} \tag{2}$$

where Q_α is the cluster charge at the beam incidence angle α and Q_0 the collected charge at perpendicular incidence. Similarly, the cluster width increases as well due to geometrical reasons. The empirical function

$$c \propto \sqrt{\tan^2\alpha + p^2} \tag{3}$$

describes the average cluster width c in terms of the number of strips contributing to the cluster with the fit parameter p, which represents the cluster width at perpendicular incidence.

Fig. 6 shows the cluster width (top) and the signal (bottom) as functions of the beam incidence angle for both pions and protons, $\alpha = 0^\circ$ denoting the perpendicular beam incidence. Fit functions (2) and (3) have been successfully applied. Due to the high ionization created by protons, the cluster spread is already more than three strips (420 μm) at perpendicular incidence.

3.7. Multi-peak mode

The APV sequencer is able to generate different programmable trigger patterns which are issued either by software or by a hardware trigger. This feature, together with the multi-peak mode of the APV25, can be used to effectively obtain subsequent samples of the shaping curve from a particle signal [7]. Fig. 7 shows an example of the APV25 output in this mode. Four triggers separated by 75 ns are sent to the APV25, which returns three consecutive samples after each trigger, resulting in a total of 12 sequential samples, revealing the (negative) pulse shape. As shown in Fig. 8, the average waveform obtained from this measurement matches with the peak mode pulse shape scanned by internal calibration.

The multi-peak mode can be used to measure the timing stability between the APV25 clock and the particle timing. For this purpose, to each event a pulse shape fit function has been applied to determine the peaking time. Using the scintillator trigger, these peaking times have been histo-

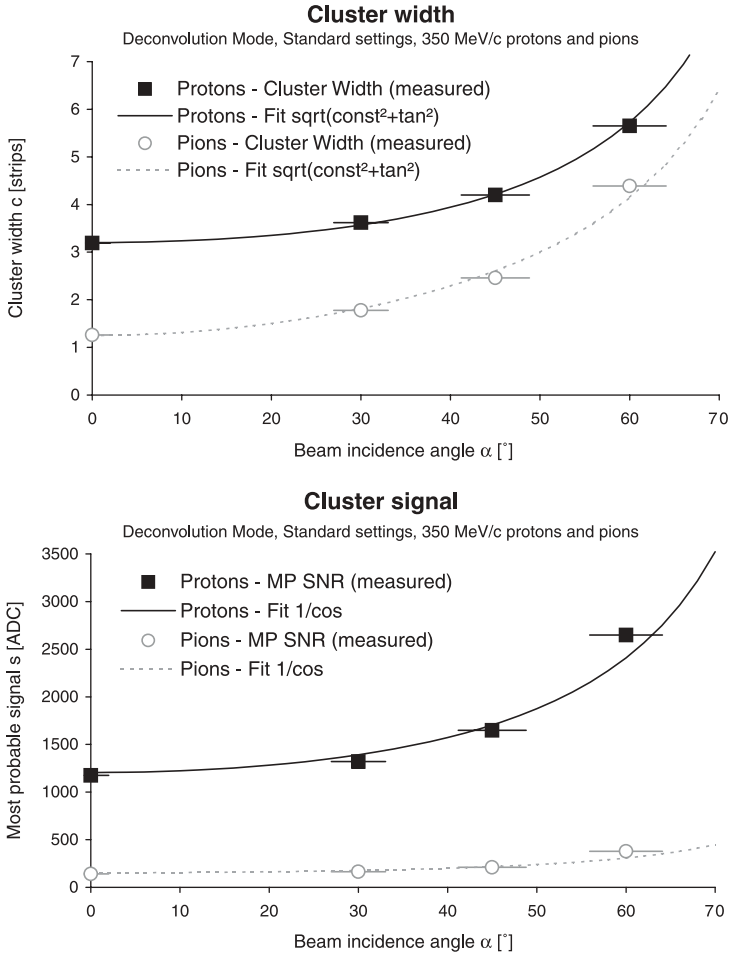

Fig. 6. Angle scan of the APV25 module. Both cluster width (top) and signal (bottom) increase with the beam incidence angle.

grammed, resulting in a Gaussian spread with an RMS of about 2 ns. This demonstrates the high precision of the system timing, although this number still includes beam fluctuations and the fit error.

At high intensity and random triggers (but necessarily synchronous to the 25 ns APV25 clock), similar Gaussian peaks appear regularly spaced in time, revealing the 20 ns bunch structure of the beam at the Paul Scherrer Institute (Fig. 9). The pulse shape fit does not always converge. With a later peak, less signal samples are contained within the measurement window, making the fit procedure more difficult. Fits which did not converge could not be included in the plot, leading to fewer entries for later peaks, although the original particle signals were evenly distributed over the full time scale.

4. Summary

For the first time a CMS silicon strip detector module has been equipped with an APV25 readout. It consisted of two high-resistivity sensors, produced from 320 μm thick 6″ wafers, and had a total strip length of 16.5 cm. This APV25 module was tested with 350 MeV c^{-1} pions and protons in a cooled environment at -10° C.

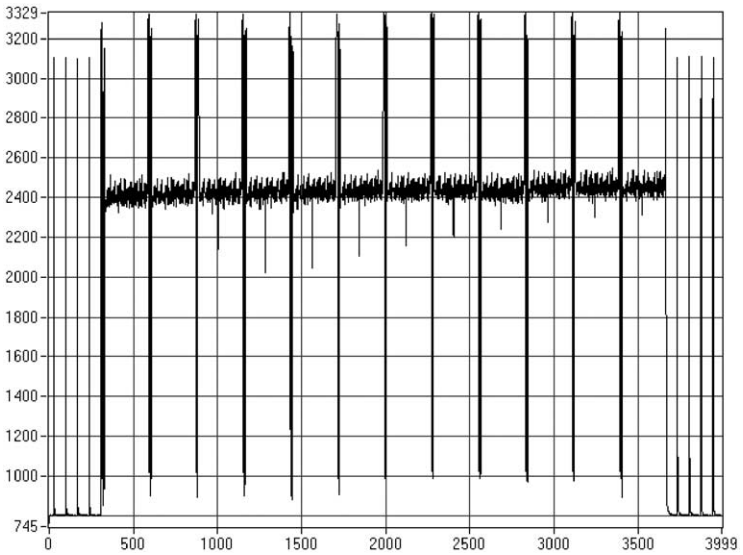

Fig. 7. Screenshot of the raw APV25 output with consecutive samples obtained with a trigger sequence in multi-peak mode, representing a single particle hit. The large spikes are header data preceding each data block.

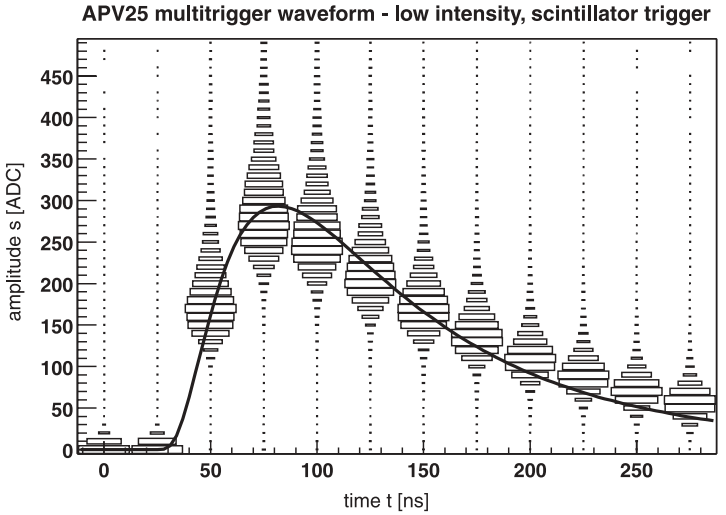

Fig. 8. Overlay of the APV25 peak mode pulse shape obtained with internal calibration and the particle signal distributions spaced by the clock period of 25 ns. The lego plots at each time slot represent Landau-like signal distributions.

The observed signal distributions for pions and protons are in agreement with the restricted energy loss in silicon predicted by the Bethe–Bloch theory. For the 350 MeV c^{-1} pions, which are approximately minimum ionizing particles, most probable SNRs of 25 and 17 were obtained in peak mode and in deconvolution mode, respectively. Thus, the APV25, which is manufactured in the 0.25 μm deep submicron process, outperforms its predecessor APV6 especially in terms of noise. The measured performance allows 25 ns bunch crossing separation with sufficient signal-to-noise

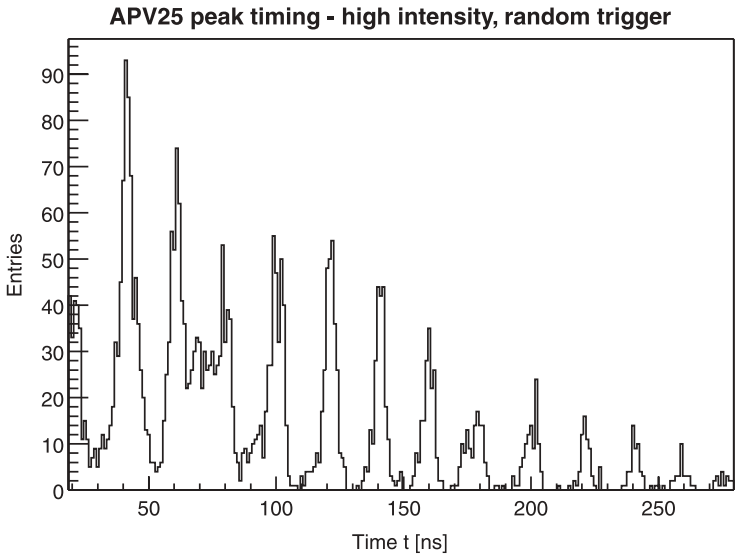

Fig. 9. APV25 peaking time distribution with random trigger at high intensity, revealing the 20 ns PSI beam period.

margin to allow excellent efficiency even with radiation-induced degradation after 10 years of LHC operation.

Moreover, a prototype of the CMS analog optical link was successfully tested in the module readout path. During a high-intensity beam period, without annealing, a radiation-induced leakage current increase was observed with a rate of $\alpha \approx 8 \times 10^{-17}$ A cm^{-1}. The cluster parameters of the measured signals at different beam incidence angles could be described by empirical functions derived from earlier measurements. Finally, the APV25 multi-peak mode has been utilized to measure a system timing precision of 2 ns RMS and to visualize the 20 ns structure of the beam with the APV25 still clocked at 25 ns.

Acknowledgements

We want to express our thanks to K. Gabathuler and to D. Renker for their help with the beamline at the Paul Scherrer Institute. Moreover, we are grateful to R. Wedenig for the wire-bonding of the silicon detector module.

References

[1] CMS Collaboration, CMS Tracker Technical Design Report, CERN/LHCC 98-6, April 1998 (http://cmsdoc.cern.ch/cms/TDR/TRACKER/tracker.html).
[2] CMS Collaboration, Addendum to the CMS Tracker TDR, CERN/LHCC 2000-016, February 2000 (http://cmsdoc.cern.ch/cms/TDR/TRACKER/tracker_addendum.pdf).
[3] L.L. Jones, et al., The APV25 Deep Submicron Chip for CMS Detectors, CERN/LHCC 99-09, September 1999, pp. 162–166 (http://www.te.rl.ac.uk/med/apv25_web/leb99_paper.pdf).
[4] M. Raymond, et al., The APV6 Readout Chip for CMS Microstrip Detectors, CERN/LHCC 97-60, September 1997 (http://www.te.rl.ac.uk/med/apv6/papers/leb_apv6_london97_paper.pdf).
[5] S. Gadomski, et al., Nucl. Instr. and Meth. A 320 (1992) 217.
[6] M. Friedl, Ph.D. Thesis, Vienna University of Technology, May 2001 (http://cern.ch/friedl → Dissertation).
[7] F. Vasey, et al., Optical links for the CMS Tracker, CERN-LHCC 99-033, October 1999 (http://cern.ch/cms-tk-opto/wdocs/leb99.pdf).
[8] T. Bauer, F. Vasey, A model for the CMS tracker analog optical link, CMS NOTE 2000/056 (http://cern.ch/cms-tk-opto/perf_pubs.html).
[9] Rose Collaboration (RD48), Third RD48 Status Report, CERN/LHCC 2000-009 (December 1999) (http://cern.ch/RD48/status-reports/RD48-3rd-status-report.pdf).
[10] W. Adam, et al., Nucl. Instr. and Meth. A 441 (2000) 427.